Mecánica Computacional Vol. XXIV
A. Larreteguy (Editor)
Buenos Aires, Argentina, Noviembre 2005

FULLY 3-WAVE MODEL TO STUDY THE HARD TRANSITION TO CHAOTIC DYNAMICS IN ALFVEN WAVE-FRONTS

Sergio A. Elaskar[*], Gonzalo Sánchez-Arriaga[+] and Juan R. Sanmartín[+]

[*]Departamento de Aeronáutica,
Universidad Nacional de Córdoba and CONICET
Av. Velez Sarfield 1611. Córdoba (5000). Argentina.
e-mail: selaskar@efn.uncor.edu

[+]Escuela Técnica Superior de Ingenieros Aeronáuticos,
Universidad Politécnica de Madrid,
Plaza Cardenal Cisneros 3, Madrid (28040), España.

Key words: DNLS – Alfvén waves – Chaos

Abstract. The derivative nonlinear Schrödinger (DNLS) equation, describing propagation of circularly polarized Alfven waves of finite amplitude in a cold plasma, is truncated to explore the coherent, weakly nonlinear coupling of three waves near resonance, one wave being linearly unstable and the other waves damped. No matter how small the growth rate of the unstable wave, the four-dimensional flow for the three wave amplitudes and a relative phase, with both resistive damping and linear Landau damping, exhibits chaotic relaxation oscillations that are absent for zero growth-rate. This hard transition in phase-space behavior occurs for left-hand (LH) polarized waves, paralleling the known fact that only LH time-harmonic solutions of the DNLS equation are modulationally unstable. The parameter domain developing chaos is much broader than the corresponding domain in a *reduced* 3-wave model that assumes equal dampings of the daughter waves.

I. Introduction

Nonlinear Alfven-wave interactions are ubiquitous in astrophysical and space plasmas. Strong nonlinear Alfven-wave effects are known to be described by the derivative nonlinear Schrödinger (DNLS) equation,[1] which admits soliton solutions[2] and has proved amenable to the inverse scattering method for obtaining general solutions[3]. A variety of behaviors allowed by the DNLS equation and its modifications have been analyzed[4]. The DNLS equation has been discussed in relation to nonlinear MHD waves observed in the Earth's bow shock[5].

A recent truncation of the DNLS equation was used to describe weakly nonlinear dynamics through the local coherent coupling of three waves near resonance (3WRI), wave 1 being linearly unstable and waves 2 and 3 equally damped (*reduced* 3WRI)[6]. This results in a three-dimensional (3D) flow of two wave amplitudes and one relative phase. Circular left-hand (LH) polarized Alfven waves exhibited a <u>hard</u> transition to complex phase-space dynamics: no matter how small the growth rate $\Gamma > 0$ of wave 1, there exists a fully developed attractor that is absent at $\Gamma \leq 0$, and is chaotic for some parametric domain. No such transition was found for right-hand polarization, paralleling the known fact that only LH time harmonic solutions of the DNLS equation are modulationally unstable[2].

In the foreshocks of Earth and Jupiter, the Alfven wave instability arises upstream from kinetic effects in ion distribution functions. A recent space example of Alfven wavefront involves orbiting conductive tethers, which, if in electrical contact with the ionosphere, radiate charge-carrying Alfven waves that close the current circuit in the ionosphere[7, 8]. Nonlinear effects at the near wavefront might be affected by the magnetic self-field generated by the very current of the tether[9]. In a possible tether experiment, a growth rate Γ could be attained by modulating the current in the tether, and thus the background magnetic field; this would excite an Alfven wave at frequency one-half the modulation frequency through certain parametric instability[10].

Here we consider the *fully* 3-wave model (different dampings, 4D flow). To keep the dimension of parameter space low we explicitly consider either resistive or linear Landau damping, for which the damping ratio for waves 2 and 3 is simply related to the respective wavenumber ratio. We want to ascertain, first, whether gross features in dynamical behavior found in the 3D flow are structurally stable (this being important because a 3WRI model may fail on a number of conditions it requires), and secondly, whether the domain in parameter space exhibiting complex dynamic behavior, and particularly chaotic behavior, is broader than in the 3D case, for which such domain is quite narrow. We will again consider the limit $\Gamma \rightarrow 0^+$.

In an early analysis, Ghosh and Papadopoulos found numerically no chaos in a *reduced* 3WRI truncation of the DNLS equation[11]. We note however that only RH polarization was discussed; also, the wavenumber ratio for waves 2 and 3 considered in Ref.12 was about unity, a case for which we did not find complex behavior with LH polarization either. A hard transition such as discussed in Ref.6 and analyzed in the present work has been found in systems other than the DNLS equation[12, 13].

II. Fully 3-wave truncation of the DNLS equation

The derivative nonlinear Schrödinger equation describes the evolution of circularly polarized Alfven waves of finite amplitude propagating along an unperturbed uniform magnetic field in a cold, homogeneous and lossless plasma, using a two-fluid, quasineutral approximation with electron inertia and current displacement neglected. Taking the unperturbed magnetic field B_0 in the z direction, the DNLS equation reads[1-4]

$$\frac{\partial \phi}{\partial t} + \frac{\partial \phi}{\partial z} \pm \frac{i}{2}\frac{\partial^2 \phi}{\partial z^2} + \frac{\partial}{\partial z}\left(\phi \frac{|\phi|^2}{4}\right) + \hat{\gamma}\,\phi \;=\; 0\,, \tag{1}$$

where ϕ, t and z are dimensionless perturbed field and variables,

$$\phi \equiv \frac{B_x \pm i\,B_y}{B_0}, \qquad \omega_{ci}\, t \;\to\; t, \qquad \frac{\omega_{ci}}{V_A} z \;\to\; z, \tag{2}$$

ω_{ci} is the ion cyclotron frequency and V_A is the Alfvén velocity. The upper (lower) sign in Eqs. (1) and (2) corresponds to a LH (RH) circularly polarized wave propagating in the z direction; we will later discuss the (growth/damping) linear operator $\hat{\gamma}$[14]. Equation (1) is derived under the following ordering scheme for perturbed quantities, $v_z/V_A \sim \Delta n/n_0 \sim (B_x/B_0)^2 \sim (B_x/B_0)^2$ (n and v_z are plasma density and velocity along the z-axis).

To study weakly nonlinear interactions, we consider an approximate solution of Eq.(1) consisting of three traveling waves satisfying a resonance condition $2k_1 = k_2 + k_3$

$$\phi \;=\; 2\sum_{j=1}^{j=3} a_j(t)\exp\left[i\psi_j(t)\right]\times \exp\left[i(k_j z - \omega_j t)\right], \tag{3}$$

with both a_j, ψ_j (in the complex amplitude) real. Wave number and frequency of modes are related by the linear (lossless) dispersion relation for circularly polarized Alfven waves at low wave number, as represented by the first three terms in (1), $\omega_j = k_j \mp k_j^{\,2}/2$.

Both the growth/damping and the nonlinear term in (1) make a_j and ψ_j vary slowly in time. Introducing (3) in Eq.(1) and neglecting all components other than k_1, k_2 and k_3 we arrive at four real equations,

$$\dot{a}_1 = -\gamma_1 a_1 - (k_2 + k_3)\, a_1\, a_2\, a_3 \sin\beta \tag{4a}$$

$$\dot{a}_2 = -\gamma_2 a_2 + k_2\, a_1^2\, a_3 \sin\beta \tag{4b}$$

$$\dot{a}_3 = -\gamma_3 a_3 + k_3\, a_1^2\, a_2 \sin\beta \tag{4c}$$

$$\dot{\beta} = \nu + \left[a_1^2 \left(k_2 \frac{a_3}{a_2} + k_3 \frac{a_2}{a_3} \right) - 2(k_2 + k_3) a_2 a_3 \right] \cos\beta - k_2\left[a_1^2 - a_2^2\right] - k_3\left[a_1^2 - a_3^2\right] \tag{4d}$$

where $\beta \equiv \pi + \nu t + \psi_2 + \psi_3 - 2\psi_1$. Note that the frequency mismatch $\nu = 2\omega_1 - \omega_2 - \omega_3$ is positive and negative for LH and RH polarization respectively. One readily finds in dimensional form,

$$\nu \approx \pm \frac{\omega_1{}^2}{\omega_{ci}} \left(\frac{k_3 - k_2}{k_3 + k_2} \right)^2 , \tag{5}$$

with $\omega_1 \approx V_a k_1$. The sign difference leads to fundamentally different dynamics for the two polarizations; in what follows we will only consider LH polarization, corresponding to positive ν.

In Eqs.(4a-d) we now set

$$a_1{}^2 \rightarrow \frac{a_1{}^2}{\sqrt{k_2\, k_3}}, \qquad a_2{}^2 \rightarrow \frac{a_2{}^2}{k_2 + k_3} \sqrt{\frac{k_2}{k_3}}, \qquad a_3{}^2 \rightarrow \frac{a_3{}^2}{k_2 + k_3} \sqrt{\frac{k_3}{k_2}} ,$$

write $\gamma_1 \equiv -\Gamma < 0$, assume $\gamma_2 < \gamma_3$, and introduce a new variable,

$$r \equiv a_3 / a_2,$$

to replace a_3. We will consider two physical models of damping. For near-parallel propagation at angle $\theta << \sqrt{2}\sqrt{\omega/\omega_{ci}}$ and non-vanishing electron temperature, linear Landau damping yields $\gamma \propto k$ and $\gamma_2/\gamma_3 = k_2/k_3 \equiv \kappa < 1$. If damping is resistive one has $\gamma \propto k^2$ and $\gamma_2/\gamma_3 = \kappa^2 < 1$ again. We then find

$$\dot{a}_1 = \Gamma a_1 - r\, a_1\, a_2^{\,2} \sin\beta, \tag{6a}$$

$$\dot{a}_2 = -\gamma_2\, a_2 + r\, a_1^{\,2}\, a_2 \sin\beta, \tag{6b}$$

$$\dot{r} = -(\gamma_3 - \gamma_2)\, r + (1 - r^2)\, a_1^{\,2} \sin\beta, \tag{6c}$$

$$\dot{\beta} = \nu - 2a_1^{\,2}\left(\bar{V} - \frac{1 + r^2}{2r}\cos\beta\right) - 2r\, a_2^{\,2}\, cos\beta + \frac{a_2^{\,2}}{2\bar{V}}\left(\kappa + \frac{r^2}{\kappa}\right), \tag{6d}$$

where

$$\bar{V} \equiv \frac{1 + \kappa}{2\sqrt{\kappa}} > 1, \qquad (\kappa \equiv k_2/k_3 < 1). \tag{7}$$

A trivial result from (6a-d) concerns the flow divergence in the 4D phase-space, reading

$$\frac{\partial}{\partial a_1^{\,2}}\frac{d\,a_1^{\,2}}{dt} + \frac{\partial}{\partial a_2^{\,2}}\frac{d\,a_2^{\,2}}{dt} + \frac{\partial}{\partial a_3^{\,2}}\frac{d\,a_3^{\,2}}{dt} + \frac{\partial}{\partial\beta}\frac{d\beta}{dt} = 2(\Gamma - \gamma_2 - \gamma_3)\,. \tag{8}$$

Nonlinear conservative coupling naturally preserves volume. For $\Gamma < \gamma_2 + \gamma_3$, as assumed here, the long-time attractor of the system will be a point-set of vanishing 3D volume.

III. The $\Gamma = 0$ attractor

Equations (6a, b) yield

$$\frac{d}{dt}\left(a_1^{\,2} + a_2^{\,2}\right) = 2\Gamma\, a_1^{\,2} - 2\gamma\, a_2^{\,2}\,. \tag{9}$$

For $\Gamma < 0$, Eq.(9) proves the equilibrium state $a_1 = a_2 = 0$ to be a global attractor, since then Eq.(6c) makes $r \to 0$. For $\Gamma > 0$, however, that equilibrium is unstable. Consider then, first, the long-time attractor of system (6a-d) at $\Gamma = 0$. Note that the entire flow is now asymptotic to the surface $a_2 = 0$, because $a_1^2 + a_2^2$ will keep diminishing in Eq.(9) unless a_2 vanishes. Since that surface is invariant, trajectories will be asymptotic to its critical elements with transverse stable manifolds.

Consider next the flow on $a_2 = 0$, where a_1 is now constant in (6a). There exists a line of fixed points Λ obtained from (6c, d) and given by

$$(\gamma_3 - \gamma_2)r = a_1^{\,2}(1 - r^2)\sin\beta\,, \tag{10a}$$

$$\nu r = a_1^{\,2}\left[2\overline{V}r - (1+r^2)\cos\beta\right]. \tag{10b}$$

Note that the value $r = 1$ would require the bracket in (10b) to vanish, which the parameter condition $\overline{V} > 1$ makes impossible. Line Λ has thus a branch Λ_l with $r < 1$, and a branch Λ_h, with $r > 1$, obtained from Λ_l by setting $r \to 1/r$, $a_1 \to a_1$ and $\beta \to 2\pi - \beta$. For Λ_l, Eqs.(10a,b) give $r = 0$, $\beta = \pi/2 + \tan^{-1}\bar{\nu}$ at $a_1 = 0$, with

$$\bar{\nu} \equiv \frac{\nu}{\gamma_3 - \gamma_2}. \tag{11}$$

As $a_1 \to \infty$ one finds $\beta \to 0$ and

$$r \to r_\infty \equiv \overline{V} - \sqrt{\overline{V}^2 - 1} \equiv \sqrt{\kappa}\,. \tag{12}$$

Finally, one can show that both $d\beta / dr$ and da_1 / dr diverge at certain value r_{max}. We find

$$r_{\max} = \sqrt{\frac{\overline{V}^2 + \bar{\nu}^2}{1 + \bar{\nu}^2}} - \sqrt{\frac{\overline{V}^2 - 1}{1 + \bar{\nu}^2}}\,, \tag{13}$$

$$\frac{a_1^{\,2}(r_{\max})}{\nu} = \frac{(1 + \bar{\nu}^2)\overline{V}}{2\bar{\nu}^2(\overline{V}^2 - 1)}, \qquad \beta(r_{\max}) = \tan^{-1}\frac{\bar{\nu}\sqrt{\overline{V}^2 - 1}}{\sqrt{\overline{V}^2 + \bar{\nu}^2}}. \tag{14a, b}$$

Both a_1 and β_l are thus double-valued functions of r between r_∞ and r_{max}. Figure 1 shows the projection of the line of fixed points on the a_1 - r plane for Landau damping and parameter values $\bar{\nu} = 1.5$, $\overline{V} = 3/2\sqrt{2}$. It may be shown that the bracket in Eq.(10b) is positive throughout Λ_l (and Λ_h); hence, Λ only exists for LH polarization.

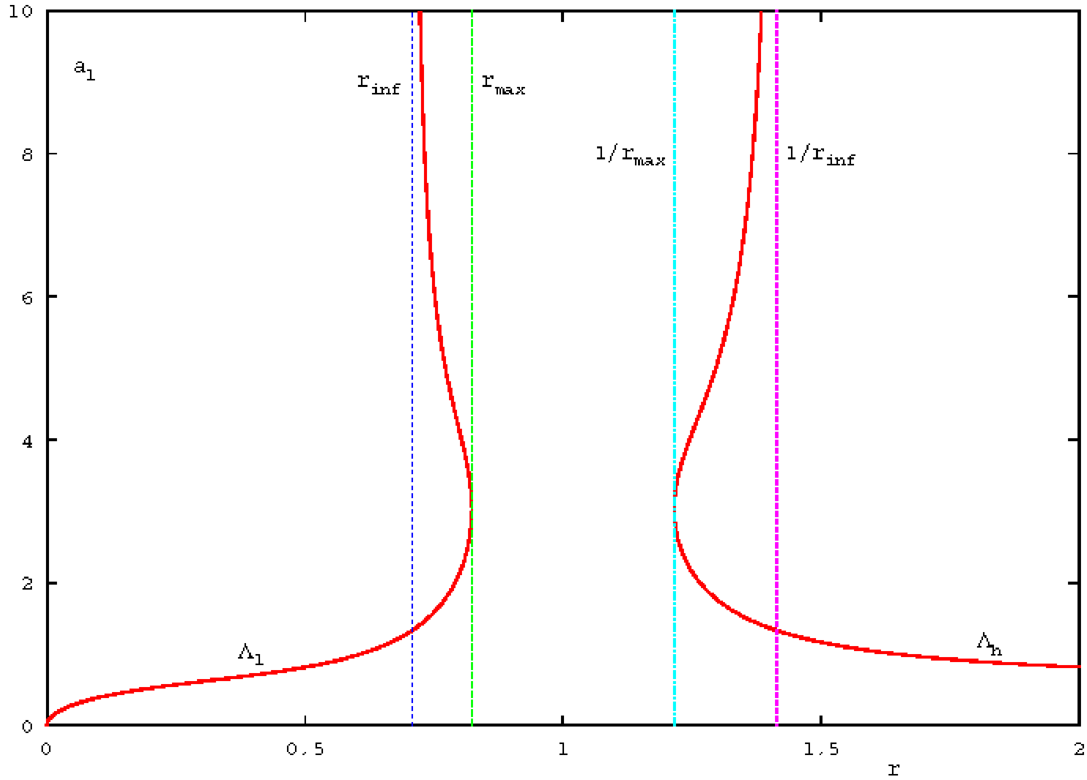

Figure 1. Projection on plane $r-a_1$ of branches Λ_l and Λ_h of the fixed points line on plane $a_2 = 0$ at $\Gamma = 0$, $\gamma_3/\gamma_2 = 2$ and $\nu = 1.5$.

Three eigenvalues of the linearized vector field at the fixed points have eigenvectors tangent to the invariant space $a_2 = 0$, determining the stability of flow on it,

$$\lambda_{1,2} = -(\gamma_3-\gamma_2)\,\frac{1+r^2}{1-r^2} \mp i\,(\nu - 2a_1^{\,2}\,\overline{V})\,\frac{1-r^2}{1+r^2}, \qquad \lambda_3 = 0, \qquad (15a, b)$$

with the null value λ_3 corresponding to an eigenvector tangent to Λ. The eigenspace associated to λ_1 and λ_2 is tangent to the invariant plane $a_1 = constant$ at the respective fixed point; as seen in (15), for flow on the space $a_2 = 0$, points on the branch Λ_l are stable and points on Λ_h are unstable. In each plane $a_1 = a_{10} < a_1(r_{max})$ within the space $a_2 = 0$ the flow is determined by Eqs.(6c, d), which describe the entire flow in the space $a_2 = 0$ moving from branch Λ_h to branch Λ_l.

The eigenvalue for stability of Λ-points off the surface $a_2 = 0$, which is the factor multiplying a_2 in Eq.(6b), $\lambda_4 = -\gamma_2 + r\,a_1^2 \sin\beta$, can be rewritten using (10a) as

$$\lambda_4 = \frac{\gamma_3 r^2 - \gamma_2}{1 - r^2}. \tag{16}$$

The associated eigenvector is transverse to the surface $a_2 = 0$ (parallel to the a_2-axis). Equation (16) shows that for motion off that surface, all points on the Λ_h branch are stable, whereas only those points on the Λ_l branch with

$$r < r_0 \equiv \sqrt{\gamma_2 / \gamma_3}\,, \tag{17}$$

are stable. Hence, for the flow in the entire 4D space, the stable fixed points of Λ are those on the $r < 1$ branch satisfying condition (17). Since, for both Landau and resistive damping, r_0 in (17) is clearly not greater than r_∞ in (12), itself less than r_{max} in (13), there always exists a point P_0 in the arc $a_1 < a_1(r_{max})$ of Λ_l having $\lambda_4 = 0$, whereas no such point exists in the arc above P_0 [i.e., $a_1 > a_1(P_0)$]. This is opposite the case for 3D, for which either both points or none existed[6]. This will lead to chaos developing over a broader domain in parametric space.

We may then conclude that, for $\Gamma = 0$, the attractor of the flow is the $a_1 < a_1(r_{max})$ Λ_l-arc below P_0 in the space $a_2 = 0$. Note that Λ_l points above P_0 have an 1D unstable manifold transverse to $a_2 = 0$, corresponding to the positive sign of the eigenvalue λ_4. There are thus singular orbits that leave that surface at those points and end on the Λ_l-points below P_0, all of which have stable manifolds transverse to $a_2 = 0$ (and lie in the $r < 1$ domain).

When Γ is made positive, there is just one fixed point P which, to lowest order in Γ, is given by $a_2^2 = \Gamma \times a_1^2/\gamma_2$, $r = \sqrt{\gamma_2/\gamma_3}$, and Eqs. (10a,b), approaching P_0 as $\Gamma \to 0$. Consider the long-time behavior of the system for Γ very small. Away from the surface $a_2 = 0$ the flow near a Λ_l-point M above P_0 will closely follow a $\Gamma = 0$ heteroclinic orbit, which will approach back to the surface $a_2 = 0$, below P_0. Because of the term Γa_1, a_1 should eventually start growing at rate Γ, keeping close to Λ_l. In terms of the eigenvalue λ_4, Eq.(6b) can be written as $da_2/dt = \lambda_4\, a_2$; since λ_4 is negative for Λ_l-points below P_0 and positive above, and the a_1-rise takes times of order $1/\Gamma$, a_2 will become exponentially small ($-\ln a_2 \sim 1/\Gamma$). Once P_0 is reached, however, a_2 will start growing; when values $a_2 \sim \sqrt{\Gamma}$ are attained, a_1 can finally reach a maximum M' and the trajectory again start separating from Λ_l.

In general, a $\Gamma \to 0^+$ attractor nested somehow around point P_0 may be described by an exact 1D map representing every maximum of $a_{1M'}$ in a trajectory within its basin of attraction, versus the preceding maximum a_{1M}. This map can be determined by a two-step algorithm. In the first step, one numerically follows the heteroclinic orbit from any point M above P_0 in Λ_l to a corresponding point m below P_0. The second step is the rise on Λ_l at vanishing rate ($t \sim 1/\Gamma$, $\Gamma \to 0$) up to the next maximum M', which can be determined by noting that, no matter how close the solution to a heteroclinic $M \to m$ orbit, Eq.(9a) will ultimately read $da_1/dt = \Gamma a_1$. With $\ln(1/a_2)$ small compared with $1/\Gamma$ at either end, and using $da_2/dt = \lambda_4 a_2$, one finally obtains

$$\gamma_2 \ln \frac{a_{1M'}}{a_{1m}} = \int_m^{M'} a_1\, r \sin\beta\, da_1 \tag{18}$$

with β and r related to a_1 through Eqs.(10a, b).

IV. $\Gamma \to 0^*$ attractors

For $\Gamma \neq 0$ the fixed point P exists only in some domain of parameter space. For Landau damping and Γ small, P does exist for

$$\left(\frac{\nu}{\gamma_2}\right)^2 \geq \frac{1+\kappa}{\kappa} \times \frac{\Gamma}{\gamma_2}, \tag{19}$$

a condition certainly satisfied everywhere for vanishing Γ, a case opposite the 3D flow. Equation (19) can be rewritten, using (5), as

$$\frac{\omega_{ci}\,\gamma_2}{\omega_1^{\,2}} \leq \frac{\sqrt{\kappa}\,(1-\kappa)^2}{(1+\kappa)^{5/2}} \times \sqrt{\frac{\gamma_2}{2\Gamma}}\ . \tag{19'}$$

Condition (19') with the equal sign is represented in Fig.2 for $\Gamma/\gamma_2 = 0.001$. Note that, because the frequency mismatch vanishes rapidly with $1 - k_2 / k_3$ in (5), $\omega_{ci}\gamma_2/\omega_1^2$ is already small at $k_2 / k_3 = 0.8$.

The fixed point P is given by the following equations:

$$r_p^2 = \frac{\gamma_2}{\gamma_3}; \qquad a_{1p}^2 = \frac{\gamma_2}{r_p \sin\beta_p}; \qquad a_{2p}^2 = \frac{\Gamma}{r_p \sin\beta_p} \tag{20}$$

$$\cos\left[\beta_p - \beta^*\right] = \frac{2\overline{V} r_p - \dfrac{1-r_p^2}{r_p}\dfrac{k}{2\overline{V}}\dfrac{\Gamma}{(\gamma_3-\gamma_2)}}{\Delta}, \tag{21}$$

where

$$\Delta = \sqrt{\frac{\nu\left(1-r_p^2\right)^2}{\left(\gamma_3-\gamma_2\right)^2} + \left[\left(1+r_p^2\right) - \frac{2\Gamma\left(1-r_p^2\right)}{\gamma_3-\gamma_2}\right]^2}\ ; \qquad (22)$$

$$\beta^* = \sin^{-1}\left[\frac{\nu\left(1-r_p^2\right)}{\Delta\left(\gamma_3-\gamma_2\right)}\right]; \qquad k = \frac{k_2}{k_3} + r_p^2\frac{k_3}{k_2} \qquad (23)$$

One can verify that for $\Gamma = 0$, the point P corresponds to point P_0, with $\lambda_3 = \lambda_4 = 0$.

The stability of P is determined by its characteristic equation, which is a fourth order polynomial involving the Jacobian matrix at P. The eigenvalues of the matrix are two couples of conjugate complex numbers. One couple, $\lambda_{1,2}$, recovers Eq.(15a) as $\Gamma \to 0$, and will have negative real parts. The other couple, λ_3 and λ_4, fully vanish in that limit, recovering (15b) and (16), with $r = r_0$. The stability of the fixed point P depends on this second couple of complex numbers. For Landau damping as assumed, one has $r_0 = \kappa$, and the analysis is considerably simplified. We represent the domain of stability of P in Fig.2 too.

Figure 3 represents the real part of eigenvalues λ_3 and λ_4 versus γ_2/γ_3 ($\equiv \kappa$ for the Landau damping case), for $\Gamma/\gamma_2 = 0.001$, and several values of ν/γ_2, with $\gamma_2 = 1$. We note that instability at a low γ_2/γ_3 ratio is present for all ν; for some ν values, however, there is instability at high γ_2/γ_3 too.

For case ν =1.5 in particular, λ_3 and λ_4 have zero real part at $\gamma_2/\gamma_3 = \kappa \approx 0.24$ and 0.71. The first case corresponds to a value $\omega_{ci}\gamma_2/\omega_1^2 \approx 0.25$ in Eq.(5). A zoom in of Fig.2 readily verify that the point does lie on curve B. The second case corresponds to a value $\omega_{ci}\gamma_2/\omega_1^2 \approx 0.039$, which lies very close to the horizontal axis, away from curve B and apparently well in the stable domain. A new zoom in of Fig.2, however, shows the interesting result that a very narrow strip, right by the γ_2/γ_3 axis, is an instability domain too.

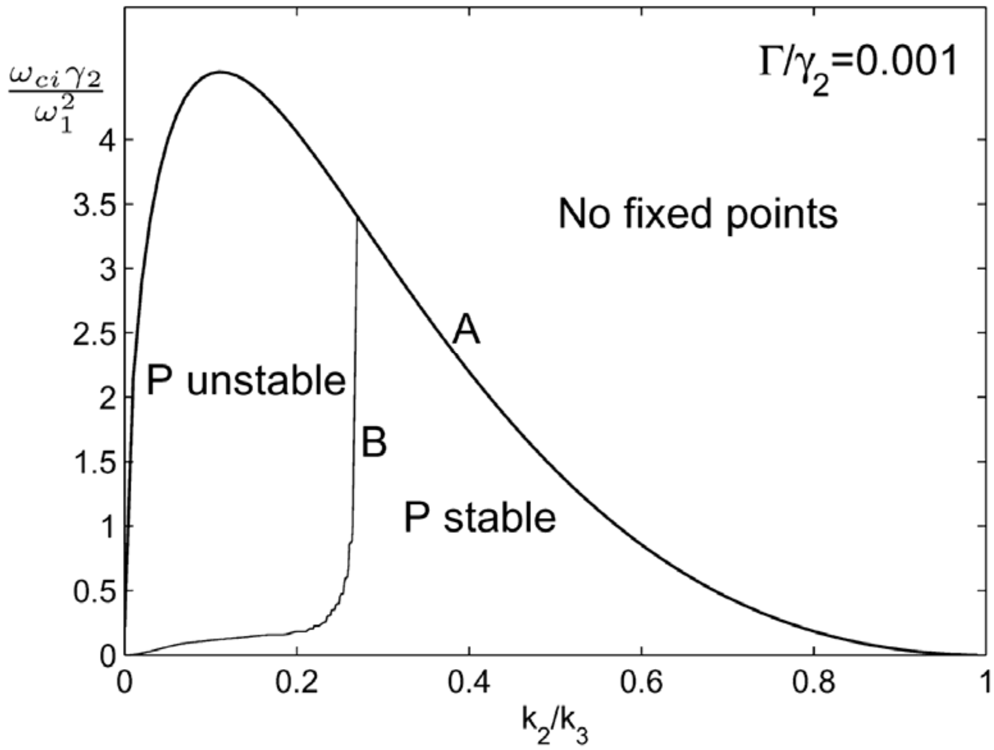

Figure 2: Stability dominion of fixed point *P*.

To study the long time dynamics behavior of the system we utilize numerical integration of the Eqs. (6a-d) using a single step, 8^{th} order Runge-Kutta method[15]. For ν = 1.5 exists two instability zones. The lost of the stability of the fixed point P presents two different behaviors in function on γ_2/γ_3. We analyze the long-time system attractors for $\gamma_2/\gamma_3 \geq 0.7$. The fixed point losses the stability approximately for γ_2/γ_3 = 0.714285714, then a periodic orbit is born through a Hopf bifurcation. As γ_2/γ_3 increases, the periodic orbit losses stability. Numerical integration of Eqs. (6a-d) shows a period-doubling cascade reaches to the appearance of a chaotic attractor for, approximately, γ_2/γ_3= 0.99960016. Figure 4 indicate the projection on space $\beta - a_2 - a_1$ of the limit cycle and the curve Λ_l for $\gamma_2/\gamma_3 = 0.99957616$. In Figure 5 is shown the projection on space $\beta - r - a_1$ of the 4-periodic orbit for $\gamma_2/\gamma_3 = 0.999580176$. The chaotic attractor for $\gamma_2/\gamma_3 = 0.999655012$ is presented in Figures 6 and 7a,b. The behavior represented in these pictures does not entail in contradiction with Eq. (9), for $\Gamma \to 0^+$ the system lounges in the neighborhood of Λ_l

for a time of order of $1/\Gamma$ ($\dot{a}_1 \approx \Gamma a_1$), with a_2 and $a_3 = r\,a_2$ exponentially small for the most that time, and $\Gamma a_1^2 - \gamma_2 a_2^2 - \gamma_3 a_3^2 \approx \Gamma a_1^2$.

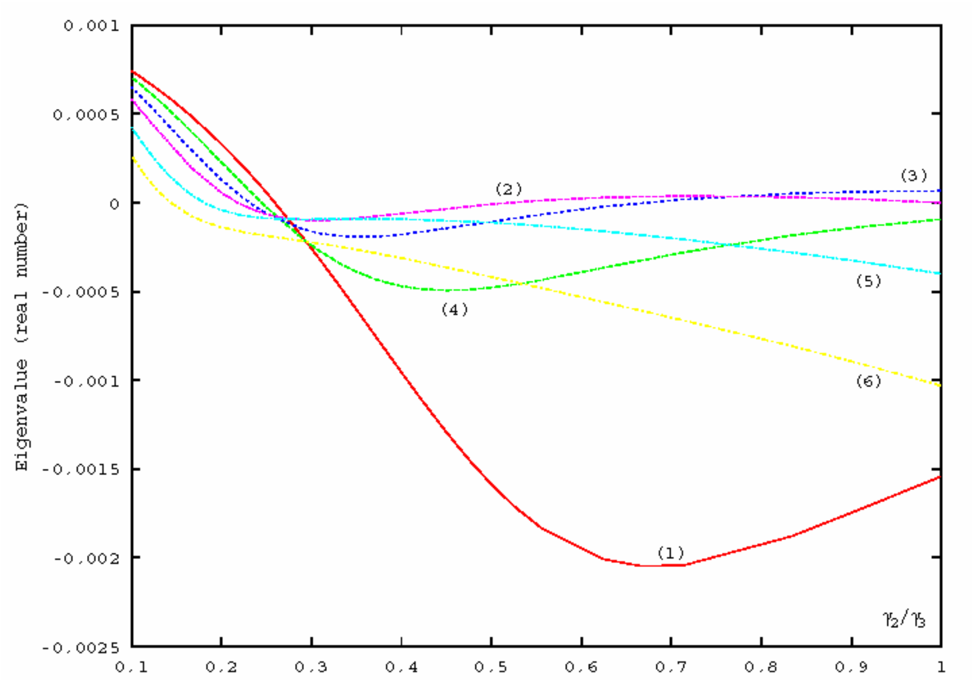

Figure 3: Stability curves. Real part of the eigenvalues in function of γ_2/γ_3 for different ν. (1) $\nu = 0.5$ - (2) $\nu = 1.0$, (3) $\nu = 1.5$, (4) $\nu = 2.0$ - (5) $\nu = 3.0$, (6) $\nu = 4.0$

Figure 7b shows the projection on the $\beta - a_1$ plane of the chaotic attractor and the lines Λ_l, Λ_h and Λ_{3D}; being Λ_{3D} the fixed points corresponding to reduced 3-wave model of the DNLS[6]. Because $\gamma_2/\gamma_3 = 0.999655012 \cong 1$, the 4-wave model is, approximately, reduced to 3D-wave model, curves Λ_l, Λ_h and Λ_{3D} are coincident ($r \approx 1$). For $0.8 \le r \le 1$ ($a_2 \approx a_3$) the projection on $\beta - a_1$ of the 4D chaotic attractor shows periodic orbits like to 3D chaotic attractor projection[6].

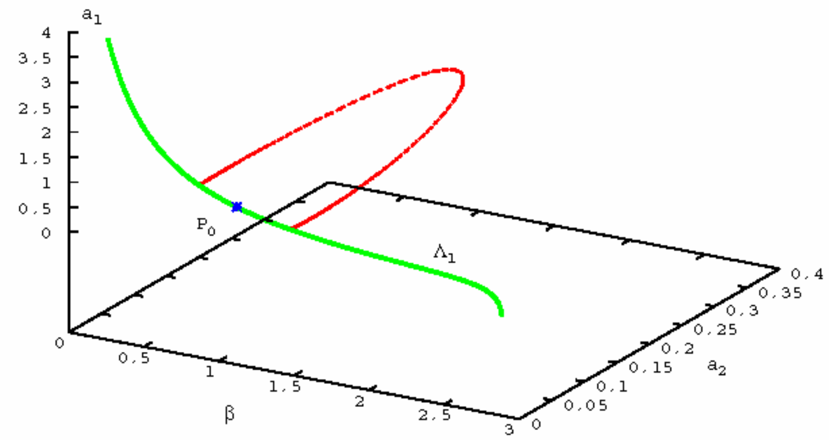

Figure 4. Projection on space $\beta - a_2 - a_1$ of the periodic orbit and the curve Λ_l for $\Gamma = 0.001$, $\gamma_2 / \gamma_3 = 0.99957616$, $\gamma_2 = 1$ and $\nu = 1.5$.

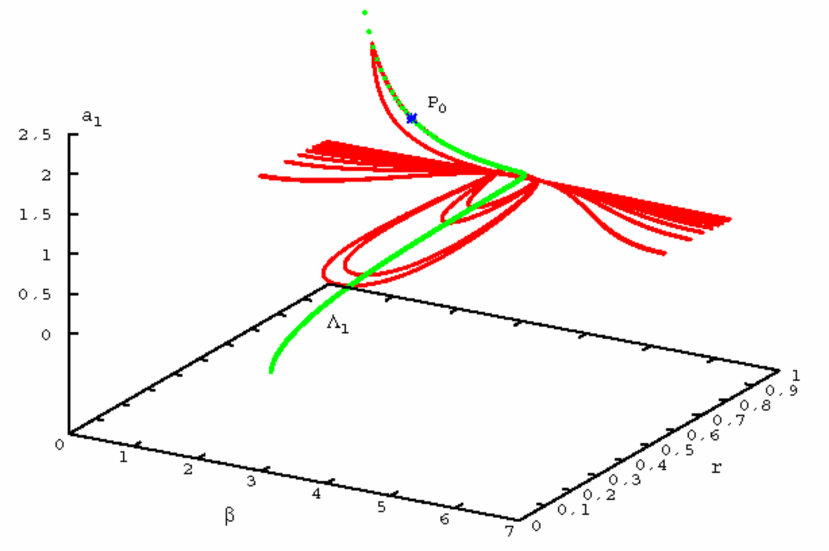

Figure 5. Projection on space $\beta - r - a_1$ of the 4-periodic orbit and the curve Λ_l for $\Gamma = 0.001$, $\gamma_2 / \gamma_3 = 0.999580176$, $\gamma_2 = 1$ and $\nu = 1.5$.

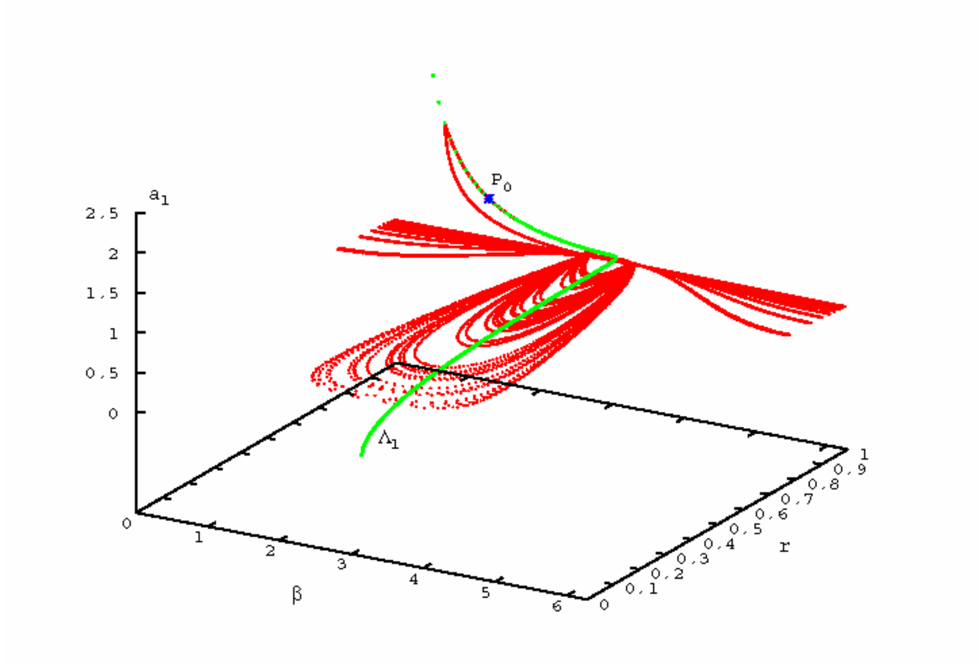

Figure 6. Projection on space $\beta - r - a_1$ of the chaotic attractor and the curve Λ_l for $\Gamma = 0.001$, $\gamma_2 / \gamma_3 = 0.999655012$, $\gamma_2 = 1$ and $\nu = 1.5$.

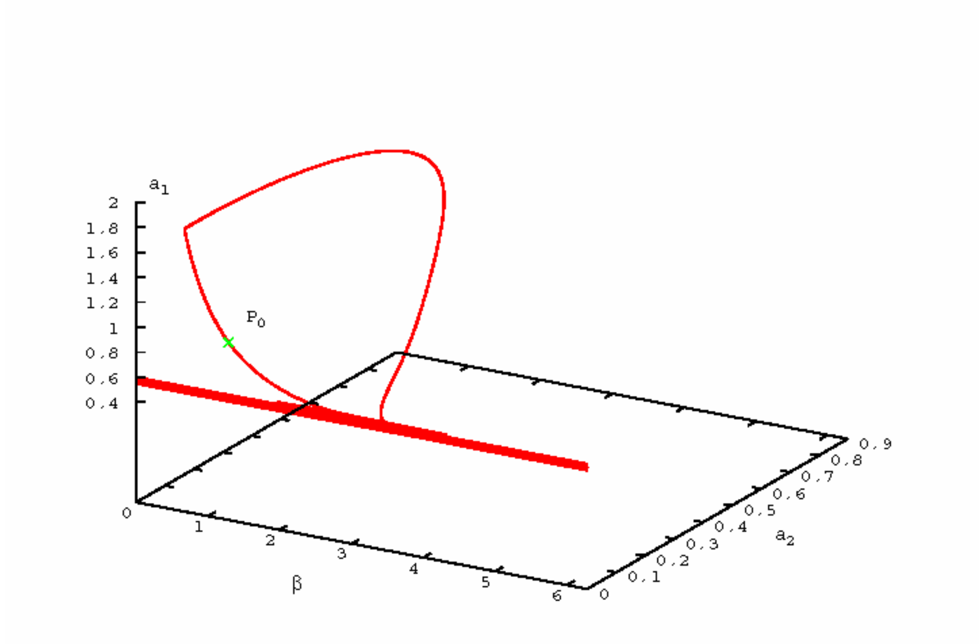

Figure 7a. Projection on space $\beta - a_2 - a_1$ of the chaotic attractor and the curve Λ_l for $\Gamma = 0.001$, $\gamma_2 / \gamma_3 = 0.999655012$, $\gamma_2 = 1$ and $\nu = 1.5$.

V. Conclusions

We have truncated the derivative nonlinear Schrödinger (DNLS) equation describing the interaction of circularly polarized Alfven waves of finite amplitude, to explore weakly nonlinear dynamics in the coherent cubic coupling of three waves near resonance (3WRI), wave 1 being linearly unstable ($\Gamma \geq 0$) and waves 2 and 3 damped, using the fully 3-wave model. We have a resulting 4D flow for amplitudes a_1, a_2, $r = a_3/a_2$ and a relative phase β.

We have found that in passing from a 3D to a 4D truncation of the DNLS equation, with realistic models of damping (either resistive or linear Landau damping) broadens considerably the domain in parameter space exhibiting chaotic behavior.

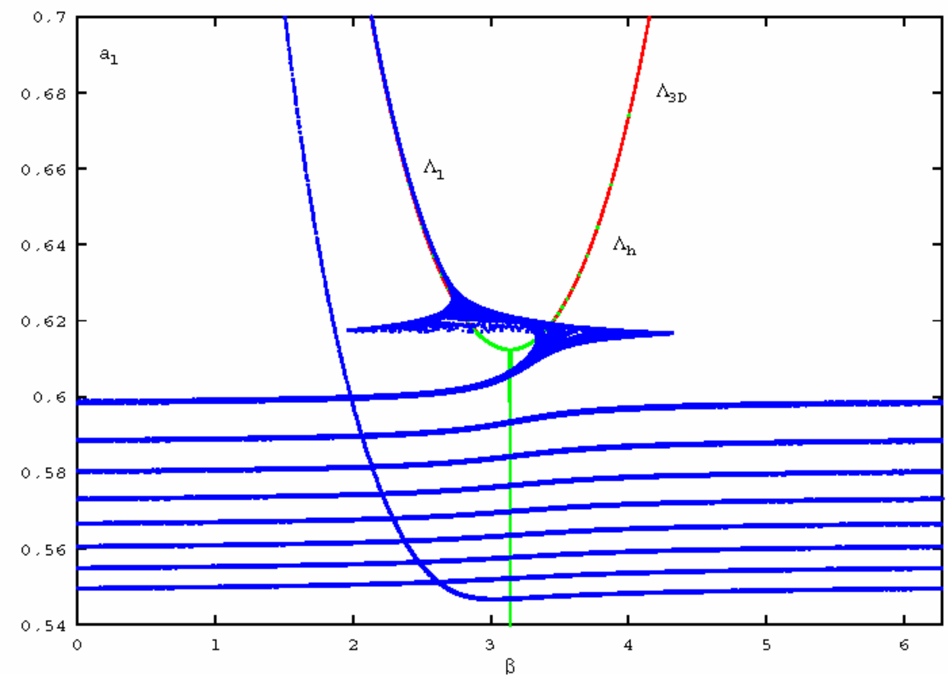

Figure 7b. Projection on space $\beta - a_1$ of the chaotic attractor, the curves Λ_l, Λ_h and Λ_{3D}. $\Gamma = 0.001$, $\gamma_2/\gamma_3 = 0.999655012$, $\gamma_2 = 1$ and $\nu = 1.5$.

Acknowledgments

This work was supported by Ministerio de Ciencia y Tecnología of Spain under Grant ESP2004-01511, by CONICET under Grant PIP 5692, FONCYT under Grant PICT-2002-10-10592 and National University of Córdoba under Grant of SECYT.

References

[1]. A.Rogister, *Phys. Fluids* **14**, 2733 (1971);

K.Mio, T.Ogino, K.Minami and S.Takeda, *J. Phys. Soc. Japan* **41**, 265 (1976).

[2]. E.Mjølhus, *J. Plasma Phys*. **16**, 321 (1976); **19**, 437 (1978).

[3]. D.J.Kaup and A.C.Newell, *J. Math. Phys.* **19**, 798 (1978).

[4]. S.R.Spangler and J.P.Sheerin, *J. Plasma Phys*. **27**, 193 (1982);

T.Hada, C.F.Kennel and B.Buti, *J.Geophys. Research* **94**, 65 (1989);

M.V.Medvedev and P.H.Diamond, *Phys. Plasmas* **3**, 863 (1996);

T.Passot and P.L.Sulem, *Phys. Plasmas* **10**, 3887 (2003).

[5]. S.R.Spangler, in *Nonlinear Waves and Chaos in Space Plasmas* (eds. T.Hada and H.Matsumoto, Terrapub, Tokyo,1997), p.171;

E.Mjølhus and T.Hada, ibidem, p.121.

[6]. J.R.Sanmartin, O. Lopez-Rebollal, E. del Rio and S. Elaskar, *Phys. Plasmas* **11**, 2026 (2004).

[7]. S.D.Drell, H.M.Foley and M.A.Ruderman, *J. Geophys. Res*. **70,** 3131 (1965);

A.Barnett and S.Olbert, *J. Geophys. Res*. **91**, 10117 (1986);

J.R.Sanmartín and M.Martínez-Sanchez, *J. Geophys. Res.* **100**, 1677 (1995).

[8]. J.R.Sanmartin and R.D.Estes, *J. Geophys. Res.* **102**, 14625 (1997).

[9]. G.V.Khazanov, N.H.Stone, E.N.Krivorutsky and E.W.Liemohn, *J. Geophys. Res.* **105**, 15835 (2000);

G.V.Khazanov, N.H.Stone, E.N.Krivorutsky, K.V.Gamayunov and E.W.Liemohn, *J. Geophys. Res.* **106**, 10565 (2001);

J.R.Sanmartin and R.D.Estes, *J. Geophys. Res.* **107**, SIA 2-1 (2002).

[10]. G.Vahala and D.Montgomery, *Phys. Fluids* **14**, 1137 (1971);

N.F.Cramer, *Plasma Phys.* **17**, 967 (1975);

M.P.Hertzberg, N.F.Cramer and S.V.Vladimirov, *Phys. Plasmas* **10**, 3160 (2003).

[11]. S. Ghosh and K. Papadopoulos, *Phys. Fluids* **30**, 1371 (1987).

[12]. D.W.Hughes and M.R.E.Proctor, *Physica D* **46**, 163 (1990);

J.R.Sanmartín, O.López-Rebollal, and N.de Paola, *Physica D* **69**, 148 (1993);

O.López-Rebollal and J.R.Sanmartín, *Physica D* **89**, 204 (1995);

E. del Río, J.R.Sanmartín, and O.López-Rebollal, *Int. J. Bifurcations and Chaos* **8**, 2255 (1998).

[13]. D.W.Hughes and M.R.E.Proctor, *Wave Motion* **20**, 201 (1994);

O.López-Rebollal, J.R.Sanmartín and E. del Río, *Phys. Plasmas* **5**, 2861 (1998).

[14]. M.I.Rabinovich and A.L.Fabrikant, *Sov. Phys. JETP* **50**, 311 (1979);

D.A.Russell and E.Ott, *Phys. Fluids* **24**, 1976 (1981).

[15]. E. B. Shanks, *Math. Comp.* **20**, 21-38 (1966).